
Porous Graphene Materials for Energy Storage and Conversion Applications

Kimal Chandula Wasalathilake, Godwin Ayoko and Cheng Yan

Additional information is available at the end of the chapter

<http://dx.doi.org/10.5772/63554>

Abstract

Porous graphene materials possess a unique structure with interconnected networks, high surface area, and high pore volume. Because of the combination of its remarkable architecture and intrinsic properties, such as high mechanical strength, excellent electrical conductivity, and good thermal stability, porous graphene has attracted tremendous attention in many fields, such as nanocomposites, lithium batteries, supercapacitors, and dye-sensitized solar cells. This chapter reviews synthesis methods, properties, and several key applications of porous graphene materials.

Keywords: porous graphene, synthesis, surface area, Li batteries, supercapacitors

1. Introduction

Porous materials are generally referred to materials containing pores or voids with different shapes and sizes. These porous structures have demonstrated unique properties and emerged as attractive candidates for a wide range of applications in medicine, catalysis, sensors, adsorbents, and energy storage and conversion [1–10]. Particularly, porous carbon is an exceptional material with a low density and high specific strength. It is also capable of bonding with other atoms through its sp , sp^2 , and sp^3 hybrid orbitals. Among various carbon materials, graphene has received enormous attention because of its high surface area ($2630 \text{ m}^2/\text{g}$), exceptional thermal conductivity (5000 W/m.K), high Young's modulus (1.0 TPa), and chemical stability. Studies have shown that it has a high intrinsic carrier mobility of $2 \times 10^5 \text{ cm}^2/\text{V.s}$ and an excellent electrical conductivity of 10^6 S/cm at room temperature [11–13]. Graphene is a

two-dimensional hexagonal lattice of sp^2 hybridized carbon atoms and since its discovery in 2004, significant efforts have been put in exploring its potential applications. Various synthesis methods have been developed to produce graphene including epitaxial growth of graphene on metal or SiC substrates [14, 15], chemical vapor deposition (CVD) [16–18], chemical reduction [19, 20], thermal reduction [21, 22], electrochemical synthesis [23, 24], and liquid phase exfoliation [25, 26]. However, because of the strong π - π stacking and van der Waals interactions between graphene sheets, the experimentally obtainable surface area is far below the theoretical value. To overcome this problem, increasing effort has been put to transforming graphene into porous structures to achieve higher surface area [27–29]. Along with the inherent properties of graphene, porous graphene has a clear edge over other porous carbon materials. For example, the excellent electrical conductivity can be used as a perfect current collector for the rapid diffusion of electrons/ions while its high mechanical strength provides mechanical stability to the porous framework. These unique properties make porous graphene a highly promising material for energy storage and conversion applications like lithium-ion batteries (LIBs), lithium-sulfur (Li-S) batteries, supercapacitors, the dye-sensitized solar cells (DSSCs), and fuel cells.

2. Synthesis of porous graphene

According to the standard specified by the International Union of Pure and Applied Chemistry (IUPAC), microporous materials have pore diameters of less than 2 nm, mesoporous materials have pore diameters between 2 and 50 nm, and macroporous materials have pore diameters of greater than 50 nm. There are basically two main methods, which can be used to fabricate porous graphene materials. These are the template and template-free methods, which will be described in greater details below.

2.1. Template approach

Template synthesis is an effective method for the transformation of graphene into porous graphene. It uses various inorganic and organic structures as templates for the transformation. Depending on the required size and morphology of pores, the appropriate template could be selected. This method can be divided into two categories: (1) soft-template method and (2) hard-template method.

2.1.1. Soft-template methods

Different kinds of amphiphilic molecules, such as surfactants and copolymers are used as structure directing agents under mild operating conditions in the soft-template methods. A bottom-up approach has been used for the preparation of mesoporous materials with two-dimensional (2D) sandwich structure consisting of graphene layers and mesoporous silica with the use of cationic surfactant, cetyltrimethyl ammonium bromide (CTAB) [30]. The presence of oxygen functionalized groups makes graphene oxide (GO) sheets negatively charged. CTAB has the capability of electrostatically adsorbing and self-assembling onto the surface of negatively charged GO in alkaline solution. The GO-based silica hybrid is formed after the

hydrolysis of silicon precursor, tetraethylorthosilicate (TEOS), and removal of CTAB. Thermal annealing at high temperature gives graphene-based silica sheets. The adsorption data have indicated a high specific area of 980 m²/g. In another method, mesostructured graphene-based SnO₂ composite is prepared by hydrothermally treating a suspension of GO, CTAB, and SnCl₄ [31].

Two-dimensional ordered mesoporous carbon nanosheets have been prepared by low molecular weight phenolic resols on graphene sheets using a triblock copolymer called Pluronic F-127 as the structure-directing agent [32]. After mixing an aqueous GO dispersion with the above prepolymer, hydrothermal treatment and further thermal annealing were carried out to prepare mesoporous carbon/graphene composite. It was reported that, Brunauer-Emmett-Teller (BET) surface area decreases with increase in the GO ratio in the composite. In another case, the same hydrothermally driven low-concentration micelle assembly approach was used with the help of anodic aluminum oxide (AAO) membranes to provide a large surface area [33]. After the hydrothermal treatment, AAO membrane was carbonized at 400–500°C for 2 h in argon atmosphere, followed by further carbonization at 700°C for 2 h in the same environment. Finally, mesoporous graphene sheets were obtained by dissolving the AAO substrate (**Figure 1**). The TEM images suggest that these nanosheets displayed ordered mesostructures, having an average pore size of 9 nm and wall thickness of 4 nm. Wen et al. [34] used a dual template method with Pluronic F-127 as the soft template and SiO₂ as the hard template to fabricate three-dimensional graphene-based hierarchically porous carbon (3DGHPC). Carbonization was carried out to convert the layer of coated polymers on SiO₂ spheres to carbon phase and simultaneously reduce GO. Finally, the 3DGHPC was obtained by treating as-prepared composite with 10% HCl to remove the SiO₂ template followed by plenty of washing with Deionized (DI) water and drying at 50°C for 24 h. The as-prepared 3DGHPC displayed a specific area of 384.4 m²/g with a pore volume of 0.73 cm³/g.

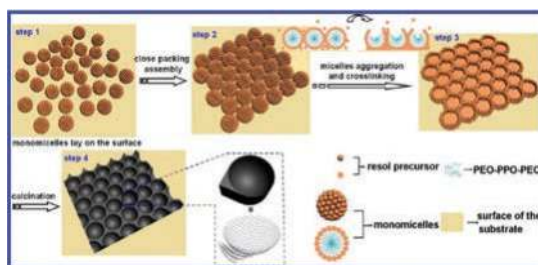


Figure 1. Schematic representation of the formation of ordered mesoporous graphene nanosheets [33]. Reprinted with the permission of the American Chemical Society.

2.1.2. Hard-template methods

When preparing porous graphene by hard template method, the template should initially be prepared. This includes the preparation of hard template itself and functionalization of its

surface to get the required properties. Then, depending on the requirement, the template should be coated with graphene or GO. The final step is the selective removal of the template without destroying its structure.

Huang et al. [35] used methyl group grafted silica spheres as a hard template to prepare nanoporous graphene foams. These graphene foams had pore sizes of 30–120 nm and ultrahigh pore volumes of 4.3 cm³/g. The surface area was reported to be 851 m²/g. Hydrophobic surface of methyl group grafted silica spheres interacts with the hydrophobic basal planes of GO to induce self-assembled lamellar like structures. Choi et al. [36] were able to use polystyrene (PS) colloidal particles as sacrificial templates to synthesize macroporous embossed chemically modified graphene (CMG) sheets with an average pore size of 2 μm. Initially, free-standing PS/CMG film was made by vacuum filtration of a mixed suspension of CMG and PS. PS particles were then removed to generate 3D macropores. Three-dimensional macroscopic graphene foams (GFs) were made by the chemical vapor deposition (CVD) method using nickel (Ni) foam as the 3D scaffold template followed by the removal of the template by hot HCl [37–43]. In 2011, Cheng et al. [44] reported a flexible 3D GF using template directed CVD. The as-prepared GF had a specific surface area, up to 850 m²/g, corresponding to an average number of layers of ~3. Poly methyl methacrylate (PMMA) can be used as a hard template to prepare macroporous graphene materials. Chen et al. [45] fabricated macroporous bubble graphene film by PMMA directed ordered assembly method. GO was mixed with the PMMA suspension and vacuum filtration was conducted to make a sandwich type assembly of the PMMA spheres and GO. Composite film was then peeled off from the filter, air dried and calcinated at 800°C to remove the template and reduce GO. As-prepared macroporous graphene film has a specific surface area of 128.2 m²/g with an average pore diameter of 107.3 nm.

2.2. Template-free approach

In the template-free approach, defects are introduced in the graphene basal planes by different methods. Chemical etching or chemical activation is one such method which had been used extensively to prepare porous carbon materials. It is an effective and relatively easy method to fabricate porous graphene sheets without using any template.

Zhu et al. [46] produced porous carbon by a simple activation with KOH of microwave exfoliated GO (MEGO) and thermally exfoliated GO (TEGO). A mixture of the MEGO and KOH was thermally treated for 1 h at 800°C in a tube furnace in argon atmosphere at a pressure of 400 torr. Pores ranging from ~1 to ~10 nm were generated in the carbon matrix by the activation with KOH. The activation of carbon with KOH proceeds as, $6\text{KOH} + \text{C} \leftrightarrow 2\text{K} + 3\text{H}_2 + 2\text{K}_2\text{CO}_3$, followed by the decomposition of K₂CO₃ and reaction of K/K₂CO₃/CO₂ with carbon [46, 47].

Porous graphene hybrids can also be produced by thermally treating a mixture of graphene and porous components [48–55]. Rui et al. [48] produced a V₂O₅/rGO composite by thermal pyrolysis of a hybrid of vanadium oxide (VO) and rGO at the temperature of 350°C for 30 min under a heating rate of 10°C/min in air. In the thermal pyrolysis process, reduced VO (rVO) is converted into polycrystalline V₂O₅ porous spheres ranging from 200 to 800 nm.

Apart from using organic and inorganic species to carry out the template-free approaches to produce porous graphene, the amphiphilic nature of GO itself can also be used to fabricate foam-like structures of macroscopic graphene. The pore sizes of these 3D macroscopic structures are in the range of submicrometer to several micrometers. Because of macroscopic nature, they possess high mechanical strength, compressibility, excellent conductivity, and adsorption characteristics [56–59]. Xu et al. [60] prepared a self-assembled graphene hydrogel (SGH) by heating the GO dispersion sealed in a Teflon-lined autoclave at 180°C for 12 h. The hydrothermally reduced GO had a well-defined 3D interconnected porous network (Figure 2). The framework of SGH was assembled on partial overlapping of flexible graphene sheets because of π - π stacking interactions. The as-prepared SGH showed excellent mechanical strength and a good electrical conductivity of 5×10^3 S/cm. Later, the same research group reported a highly conductive graphene hydrogel which was reduced by hydrazine hydrate or hydrogen iodide to improve the conductivity by further removing its residual oxygenated groups [61].

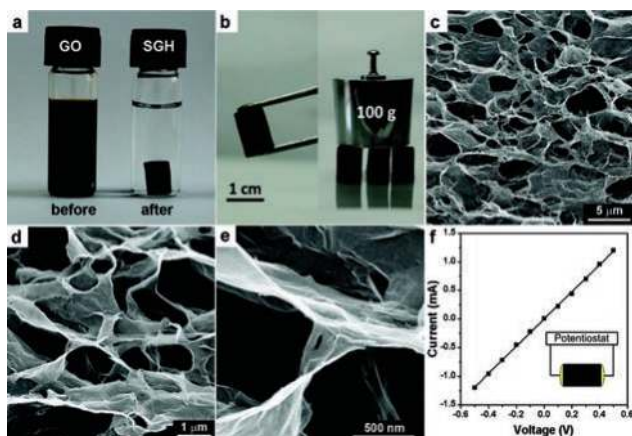


Figure 2. (a) Photographs of a 2 mg/ml homogeneous GO aqueous dispersion before and after hydrothermal reduction at 180°C for 12 h; (b) photographs of a strong SGH allowing easy handling and supporting weight; (c-e) SEM images with different magnifications of the SGH interior microstructures; (f) room temperature I - V curve of the SGH exhibiting Ohmic characteristic, inset shows the two-probe method for the conductivity measurements [60]. Reprinted with the permission of the American Chemical Society.

3. Applications of porous graphene materials

Unique porous structure of graphene along with its superior properties makes graphene a potential candidate for energy storage and conversion applications. The following sections review several key applications of porous graphene in LIBs, Li-S batteries, supercapacitors, and the dye-sensitized solar cells.

3.1. Lithium-ion batteries

Lithium-ion battery has a widespread increasing demand because of its high energy density, flexibility, low maintenance, and longer lifespan compared with other battery technologies [62]. To further increase the energy density, charging efficiency, and cycle life of lithium-ion batteries, it is essential to look at new electrode materials that have good lithium storage capability. Porous graphene with exceptional properties holds a great potential as an electrode material for the lithium-ion battery. The high surface area of graphene can significantly increase the diffusion of lithium ions and electrons. Furthermore, the superior electrical conductivity provides a good conductive network within the electrodes. Graphene can construct a 3D framework with a strong tolerance to the volume change of electrochemically active materials during charge-discharge cycles [63].

An anode material for Li-ion battery was made by hierarchical mesoporous and macroporous carbon using the spinodal decomposition of a mesophase pitch (MP) carbon precursor and polystyrene as a soft template [64]. Scanning Electron Microscope (SEM) images of this structure revealed a 3D bicontinuous network of macropores and according to Hg porosimetry the average macropore size was recorded as 100 μm . The first reversible capacity of 470 mAh/g was recorded at a discharge-charge rate of C/5. When discharge-charge rates were increased to 1 and 5 C, reversible capacities of 320 and 200 mAh/g were obtained. Yang et al. [30] managed to synthesize a graphene-based mesoporous carbon anode which performed better than previous graphitic anode. Two-dimensional sandwich like graphene structure increases the surface area while each nanosheet acts as a mini-current collector. They facilitate the rapid transportation of electrons during charge-discharge cycles. At the rate of C/5, its reversible capacity stabilized at 770 mAh/g. When the discharge-charge rates were increased to 1 and 5 C, the reversible capacities recorded 540 and 370 mAh/g, respectively.

Graphene materials loaded with macroporous structures have shown positive results as anode materials for the Li-ion batteries. Mn_3O_4 -graphene [65], Co_3O_4 -graphene [66], and Fe_3O_4 -graphene [67–69] have been studied extensively as potential anode materials for Li-ion materials. Chen et al. [69] reported a 3D graphene- Fe_3O_4 hybrid prepared by chemical reduction of the GO in the presence of Fe_3O_4 nanoparticles. The as-prepared hybrid was tested as an anode material for LiBs and exhibited capacities of 990 and 730 mAh/g at current densities of 800 and 1600 mA/g, respectively.

3.2. Li-sulfur batteries

For more than 20 years, the Li-ion battery has dominated the rechargeable battery market for portable devices and it is still the best choice for electric vehicles. But, when it comes to the electrical performance, a significant improvement is less likely as the performance of the Li-ion battery has almost reached its theoretical limits [70, 71]. Therefore, Li-S battery is considered as one of the potential candidates to replace the Li-ion battery as the next generation rechargeable battery. Sulfur is considered as the 10th most abundant element in the Earth. When employed as a cathode, it has a high specific capacity of 1675 mAh/g and it can deliver a specific energy of 2600 Wh/kg. However, several key issues have prevented the practical applications of Li-S batteries so far. The issues which need to be addressed are (i) poor electrical

conductivity of sulfur and its final discharge products ($\text{Li}_2\text{S}/\text{Li}_2\text{S}_2$); (ii) large volume change of sulfur electrode during electrochemical cycling; and (iii) dissolution of polysulfides, intermediate reactant products in the organic electrolyte leading to deposition of $\text{Li}_2\text{S}_2/\text{Li}_2\text{S}$ at the electrode interface. To overcome these drawbacks, extensive researches have been carried out to use graphene materials as scaffolds for cathodes in Li-S batteries [72–76].

For the first time, Wang et al. [77] synthesized a sulfur-graphene (S-GNS) composite by heating a mixture of graphene nanosheets and elemental sulfur. The electrochemical performance of the battery was unsatisfactory as S-GNS electrode contained only 17.6 wt% sulfur. Wang et al. [78] improved the performance of this cathode by increasing the sulfur content up to 44.5 wt % using the same synthesis method. The reversible capacities of the electrode were recorded as 662 mAh/g at 1 C and 391 mAh/g at 2 C after 100 cycles.

Kim et al. [79] produced mesoporous graphene-silica composite (m-GS) as a cathode structure to host sulfur for Li-S batteries. With the help of the ternary cooperative assembly of triblock copolymer (P123), silica precursor and graphene, porous silica structure was made parallel to graphene sheets. Sulfur was infiltrated into the mesoporous structure by melt diffusion at 155°C for 12 h. S intercalated graphite oxide cathode was made by in situ sulfur reduction and intercalation of graphite oxide [80]. By heating a mixture of S_8 and graphite oxide at 600°C under vacuum, would break large molecules of S_8 into S_2 and in the meantime reduce graphite oxide to graphene. Interplanar distance of the carbon matrix allows S_2 to intercalate into GO. To minimize the capacity decay, surface S_8 could be removed by CS_2 . This specified cathode was able to maintain a reversible capacity of 880 mAh/g after 200 cycles.

To obtain better electrochemical performance, Zhang et al. [81] created dense nanopores on the surface of graphene nanosheets by chemically activating hydrothermally reduced graphene oxide (rGO). Sulfur was infiltrated into the KOH-activated graphene hydrogels by the melt diffusion method (Figure 3). The rGO hydrogel served as a trap for soluble polysulfides.

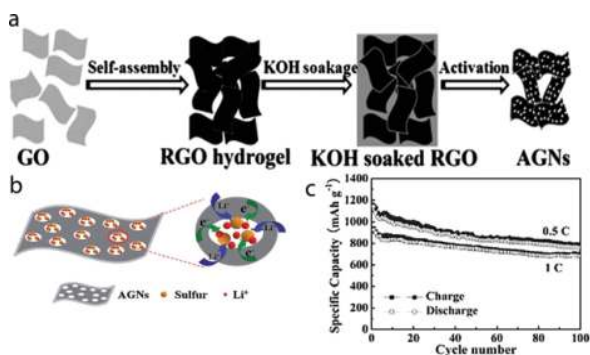


Figure 3. (a) Schematic representation of the preparation route of activated graphene nanosheets through self-assembly of GO, ion diffusion and chemical activation strategy. (b) Proposed scheme for the constrained electrochemical reaction process of the graphene/sulfur composite. (c) Cycling performances of graphene/sulfur composite electrode at 0.5 C and 1 C [81]. Reprinted with the permission of the Royal Society of Chemistry.

According to results from nitrogen sorption measurements, the surface area of the mesoporous system was 2313 m²/g and the mean value of nanopores was 3.8 nm. At 0.5 C and 1 C, the graphene/sulfur composite electrode delivered high reversible capacities of 1143 and 927 mAh/g, respectively.

Evers and Nazar [82] prepared a graphene-sulfur cathode material with a sulfur loading of 87 wt% by a simple one pot method. A mixture of GO and soluble polysulfide was oxidized *in situ* as a one pot reaction. Because of the formation of insulating Li₂S layer, the initial discharge capacity of 705 mAh/g at 0.2 C decreased drastically after 50 cycles. S/rGO composite material for Li-S battery cathode was made by concurrently oxidizing sulfide and reducing GO [83]. In this method, Na₂S and Na₂SO₃ were mixed with the GO solution. The composite material is obtained by the reduction of GO by Na₂S. The composite with a sulfur loading of 63.6 wt% delivered a reversible capacity of 804 mAh/g after 80 cycles at 0.186 C and 440 mAh/g after 500 cycles at 0.75 C. Gao et al. [84] prepared a sulfur cathode composed of sulfur nanoparticles wrapped in graphene by using Na₂S₂O₃ as a precursor of sulfur. In acidic medium, Na₂S₂O₃ can also serve as a reducing agent of GO. Polyvinylpyrrolidone (PVP) was used to prevent the S particles from aggregation and to keep the sulfur particles at submicrometer range. By using (NH₄)₂S₂O₃ as a sulfur precursor, Xu et al. made a graphene-encapsulated sulfur composite. In this synthesis method, a mild reducing agent, urea, was used to reduce GO.

3.3. Supercapacitors

Supercapacitor is another major alternative solution for the energy storage applications. Supercapacitors have higher power densities than batteries and also higher energy densities than dielectric capacitors [46, 85–88]. The first attempt to use graphene as a supercapacitor was done by Rouff et al. [89] in 2008. In that method, GO was reduced by using hydrazine hydrate and the surface area as measured by BET method was 705 m²/g. Specific capacitances of 135 and 99 F/g were obtained in aqueous and organic electrolytes, respectively. However, strong π - π stacking and van der Waals attractions among inter layers cause irreversible agglomeration to form graphite, resulting a decrease in surface area which may hinder the diffusion of the electrolyte. Therefore, making graphene in to a highly open porous structure is an effective way to increase the accessible surface area and the specific capacitance.

Zhu et al. [46] were able to make a carbon based supercapacitor by chemically activating the microwave exfoliated GO (MEGO) and thermally exfoliated GO (TEGO) using the KOH to obtain surface area values up to 3100 m²/g and a high electrical conductivity of 500 S/m with a C/O atomic ratio of 35. The specific capacitance values calculated from the charge-discharge curves were 165, 166, and 166 F/g at current densities of 1.4, 2.8, and 5.7 A/g, respectively.

Chen et al. [90] discovered a route to convert noncovalent functionalized graphene to a graphene-activated carbon composite by chemically activating with the KOH, which consisted of a specific surface area of 798 m²/g. Stable graphene colloids absorbed by oligomers of p-phenylene diamine (PPD) were converted to a graphene-activated carbon composite by the KOH activation annealing method. The KOH activation created micro/mesopores in the

activated carbon covered on graphene whereas pores in activated carbon also contributed the high surface area of the composite. The as-prepared graphene composite exhibited a specific capacitance of 122 F/g and energy density of 6.1 Wh/kg in aqueous electrolyte. Maximum energy density values of 52.2 and 99.2 Wh/kg were obtained in 1-ethyl-3-methylimidazolium tetrafluoroborate (EMIMBF₄) electrolyte at room temperature and 80°C, respectively.

Zhang et al. [91] introduced a method to produce porous 3D graphene-based bulk materials with ultrahigh specific area of 3523 m²/g and excellent bulk conductivity (up to 303 S/m) by *in-situ* hydrothermal polymerization/carbonization of a mixture of industry carbon sources and the GO followed by KOH activation (Figure 4). The carbon sources used in this method were biomass, phenol-formaldehyde (PF), polyvinyl alcohol (PVA), sucrose, cellulose, and lignin. Graphene-PF composite material gave the highest specific capacitance values of 202 F/g in 1 M TEABF₄/AN and 231 F/g in neat EMIMBF₄ electrolyte systems, respectively.

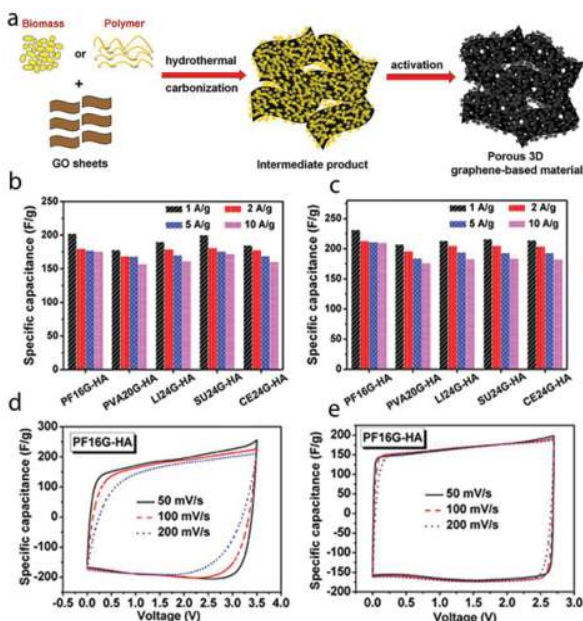


Figure 4. (a) Schematic representation of the synthesis procedure of the porous three-dimensional graphene-based materials. Galvanostatic charge/discharge test results of supercapacitors based on the optimized porous 3D graphene-based materials in (b) 1 M TEABF₄/AN and (c) neat EMIMBF₄ electrolytes under different current densities. CV curves of PF16G-HA based supercapacitor under different scan rates in (d) 1 MTEABF₄/AN and (e) neat EMIMBF₄ electrolyte. Reproduced with permission [91], Copyright 2013 NPG.

The electrochemical performance of carbon based materials can be enhanced by doping carbon network with nitrogen and boron [92–95]. Nitrogen and boron co-doped 3D graphene aerogel

(BN-GA) was fabricated by using the GO and ammonia boron trifluoride (NH_3BF_3) [96]. The interconnected framework of graphene nanosheets had a surface area of $249 \text{ m}^2/\text{g}$ with a macroporous structure. BN-GAs were directly processed into thin electrodes without destroying the 3D continuous frameworks and used in all-solid-state supercapacitors (ASSSs). Because of the unique structure and strong synergetic effects of nitrogen and boron co-doping, a specific capacitance of 62 F/g and energy density of 8.65 Wh/kg were obtained. 3D graphene aerogels with mesoporous silica frameworks (GA- SiO_2) were fabricated by the hydrolysis of TEOS with graphene aerogel and CTAB as the soft template [97]. Graphene aerogel-mesoporous carbon (GA-MC) with a surface area of $295 \text{ m}^2/\text{g}$ was generated by infiltrating a sucrose solution into the GA- SiO_2 followed by carbonization at 700°C for 3 h in argon. The as-prepared GA-MC exhibited a specific capacitance of 226 F/g when it was used as a supercapacitor.

3.4. Dye-sensitized solar cells

The dye-sensitized solar cells are among third generation photovoltaic devices that are cost-effective and highly efficient. It consists of a mesoporous TiO_2 photoanode with a dye to increase light absorption, a counter electrode (CE), and electrolyte. The CE should reduce redox species, which are used to regenerate the sensitizer after electron ejection. To increase the efficiency of DSSC, it is essential to select a CE material with low sheet resistance, high catalytic activity for the reduction of redox species, excellent chemical stability, and low cost. Recently, graphene-based CEs have been studied extensively as a potential cost-effective replacement for platinum based CEs.

Compared with other graphene-based materials, functionalized or doped graphene exhibits exceptional electrocatalytic activity. In 2012, Xu et al. prepared Hemin, an iron-containing porphyrin functionalized rGO by microwave irradiation [98]. The Hemin-rGO hybrid exhibited a power conversion efficiency (PCE) value of 2.45 %. Yen et al. [99] reported a nitrogen-doped graphene prepared using a hydrothermal method. The nitrogen-doped domains on the graphene surface act as electroactive sites, which have selectivity for redox species in the reduction reaction. The as-prepared nitrogen-doped graphene CE exhibited the PCE value of 4.75%. Xue et al. [100] managed to prepare 3D nitrogen-doped graphene foams with a nitrogen content of 7.6% freeze drying the GO foams followed by annealing at 800°C in ammonia/argon mixture for 1 h. Because of the high content of nitrogen, the PCE value of 7.07% was obtained.

4. Conclusion

In conclusion, owing to its high surface area, unique pore structure, and remarkable electrochemical performances, porous graphene has attracted great attention in the fields of energy storage and conversion. However, there are several key issues, which need to be addressed. The precise control of pore size, pore morphology, and wall thickness is necessary for the assembly of hierarchically structured porous graphene materials. Introduction of different sizes of pores into graphene matrix is essential to produce porous graphene materials to obtain

synergic effects of different pores. With increasing research efforts in the field, we believe that there would be significant advances in the synthesis and application of porous graphene in the near future, benefiting development of high performance energy conversion and storage devices. This research was partially supported under the Australian Research Council Discovery Project (DP150101717). Kimal Chandula Wasalathilake acknowledges the QUTPRA scholarship from the Queensland University of Technology.

Author details

Kimal Chandula Wasalathilake, Godwin Ayoko and Cheng Yan*

*Address all correspondence to: c2.yan@qut.edu.au

School of Chemistry, Physics and Mechanical Engineering, Science and Engineering Faculty, Queensland University of Technology (QUT), Brisbane, Australia

References

- [1] Davis ME. Ordered porous materials for emerging applications. *Nature*. 2002;417(6891):813–821.
- [2] Cooper AI. Porous materials and supercritical fluids. *Advanced Materials*. 2003;15(13):1049–1059. DOI: 10.1002/adma.200300380.
- [3] Zhang H, Cooper AI. Synthesis and applications of emulsion-templated porous materials. *Soft Matter*. 2005;1(2):107–113. DOI: 10.1039/B502551F.
- [4] Lee J, Kim J, Hyeon T. Recent progress in the synthesis of porous carbon materials. *Advanced Materials*. 2006;18(16):2073–2094. DOI: 10.1002/adma.200501576.
- [5] Lu AH, Schüth F. Nanocasting: a versatile strategy for creating nanostructured porous materials. *Advanced Materials*. 2006;18(14):1793–1805. DOI: 10.1002/adma.200600148.
- [6] White RJ, Budarin V, Luque R, Clark JH, Macquarrie DJ. Tuneable porous carbonaceous materials from renewable resources. *Chemical Society Reviews*. 2009;38(12):3401–3418. DOI: 10.1039/B822668G.
- [7] White RJ, Luque R, Budarin VL, Clark JH, Macquarrie DJ. Supported metal nanoparticles on porous materials. Methods and applications. *Chemical Society Reviews*. 2009;38(2):481–494. DOI: 10.1039/B802654H.
- [8] Thomas A. Functional materials: from hard to soft porous frameworks. *Angewandte Chemie International Edition*. 2010;49(45):8328–8344. DOI: 10.1002/anie.201000167.

- [9] Bae Y-S, Snurr RQ. Development and evaluation of porous materials for carbon dioxide separation and capture. *Angewandte Chemie International Edition*. 2011;50(49):11586–11596. DOI: 10.1002/anie.201101891.
- [10] Boissiere C, Grosso D, Chaumonnot A, Nicole L, Sanchez C. Aerosol route to functional nanostructured inorganic and hybrid porous materials. *Advanced Materials*. 2011;23(5):599–623. DOI: 10.1002/adma.201001410.
- [11] Geim AK, Novoselov KS. The rise of graphene. *Nature Material* 2007;6(3):183–191.
- [12] Geim AK. Graphene: status and prospects. *Science*. 2009;324(5934):1530–1534. DOI: 10.1126/science.1158877.
- [13] Novoselov KS, Falco VI, Colombo L, Gellert PR, Schwab MG, Kim K. A roadmap for graphene. *Nature*. 2012;490(7419):192–200.
- [14] Berger C, Song Z, Li T, Li X, Ogbazghi AY, Feng R, Dai Z, Marchenkov AN, Conrad EH, First PN, de Heer WA. Ultrathin epitaxial graphite: 2D electron gas properties and a route toward graphene-based nanoelectronics. *The Journal of Physical Chemistry B*. 2004;108(52):19912–19916. DOI: 10.1021/jp040650f.
- [15] Edwards RS, Coleman KS. Graphene film growth on polycrystalline metals. *Accounts of Chemical Research*. 2013;46(1):23–30. DOI: 10.1021/ar3001266.
- [16] Wu B, Geng D, Guo Y, Huang L, Xue Y, Zheng J, Chen J, Yu G, Liu Y, Jiang L, Hu W. Equiangular hexagon-shape-controlled synthesis of graphene on copper surface. *Advanced Materials*. 2011;23(31):3522–3525. DOI: 10.1002/adma.201101746.
- [17] Xue Y, Wu B, Jiang L, Guo Y, Huang L, Chen J, Tan J, Geng D, Luo B, Hu W, Yu G, Liu Y. Low temperature growth of highly nitrogen-doped single crystal graphene arrays by chemical vapor deposition. *Journal of the American Chemical Society*. 2012;134(27):11060–11063. DOI: 10.1021/ja302483t.
- [18] Li X, Cai W, An J, Kim S, Nah J, Yang D, Piner R, Velamakanni A, Jung I, Tutuc E, Banerjee SK, Colombo L, Ruoff RS. Large-area synthesis of high-quality and uniform graphene films on copper foils. *Science*. 2009;324(5932):1312–1314. DOI: 10.1126/science.1171245.
- [19] Pei S, Cheng H-M. The reduction of graphene oxide. *Carbon*. 2012;50(9):3210–3228. DOI: <http://dx.doi.org/10.1016/j.carbon.2011.11.010>.
- [20] Park S, Ruoff RS. Chemical methods for the production of graphenes. *Nature Nano*. 2009;4(4):217–224.
- [21] Zhang C, Lv W, Xie X, Tang D, Liu C, Yang Q-H. Towards low temperature thermal exfoliation of graphite oxide for graphene production. *Carbon*. 2013;62:11–24. DOI: <http://dx.doi.org/10.1016/j.carbon.2013.05.033>.

- [22] Liu Y-Z, Chen C-M, Li Y-F, Li X-M, Kong Q-Q, Wang M-Z. Crumpled reduced graphene oxide by flame-induced reduction of graphite oxide for supercapacitive energy storage. *Journal of Materials Chemistry A*. 2014;2(16):5730–5737. DOI: 10.1039/C3TA15082H.
- [23] Liu J, Yang H, Zhen SG, Poh CK, Chaurasia A, Luo J, Wu X, Yeow EKL, Sahoo NG, Lin J, Shen Z. A green approach to the synthesis of high-quality graphene oxide flakes via electrochemical exfoliation of pencil core. *RSC Advances*. 2013;3(29):11745–11750. DOI: 10.1039/C3RA41366G.
- [24] Zhao M-Q, Zhang Q, Huang J-Q, Wei F. Hierarchical nanocomposites derived from nanocarbons and layered double hydroxides – properties, synthesis, and applications. *Advanced Functional Materials*. 2012;22(4):675–694. DOI: 10.1002/adfm.201102222.
- [25] Cui X, Zhang C, Hao R, Hou Y. Liquid-phase exfoliation, functionalization and applications of graphene. *Nanoscale*. 2011;3(5):2118–2126. DOI: 10.1039/C1NR10127G.
- [26] Nicolosi V, Chhowalla M, Kanatzidis MG, Strano MS, Coleman JN. Liquid exfoliation of layered materials. *Science*. 2013;340(6139). DOI: 10.1126/science.1226419–18.
- [27] Han S, Wu D, Li S, Zhang F, Feng X. Porous graphene materials for advanced electrochemical energy storage and conversion devices. *Advanced Materials*. 2014;26(6):849–864. DOI: 10.1002/adma.201303115.
- [28] Jiang L, Fan Z. Design of advanced porous graphene materials: from graphene nanomesh to 3D architectures. *Nanoscale*. 2014;6(4):1922–1945. DOI: 10.1039/C3NR04555B.
- [29] Yan Z, Yao W, Hu L, Liu D, Wang C, Lee C-S. Progress in the preparation and application of three-dimensional graphene-based porous nanocomposites. *Nanoscale*. 2015;7(13):5563–5577. DOI: 10.1039/C5NR00030K.
- [30] Yang S, Feng X, Wang L, Tang K, Maier J, Müllen K. Graphene-based nanosheets with a sandwich structure. *Angewandte Chemie*. 2010;122(28):4905–4909. DOI: 10.1002/ange.201001634.
- [31] Yang S, Yue W, Zhu J, Ren Y, Yang X. Graphene-based mesoporous SnO₂ with enhanced electrochemical performance for lithium-ion batteries. *Advanced Functional Materials*. 2013;23(28):3570–3576. DOI: 10.1002/adfm.201203286.
- [32] Wang L, Sun L, Tian C, Tan T, Mu G, Zhang H, Fu H. A novel soft template strategy to fabricate mesoporous carbon/graphene composites as high-performance supercapacitor electrodes. *RSC Advances*. 2012;2(22):8359–8367. DOI: 10.1039/C2RA20845H.
- [33] Fang Y, Lv Y, Che R, Wu H, Zhang X, Gu D, Zheng G, Zhao D. Two-dimensional mesoporous carbon nanosheets and their derived graphene nanosheets: synthesis and efficient lithium ion storage. *Journal of the American Chemical Society*. 2013;135(4):1524–1530. DOI: 10.1021/ja310849c.
- [34] Wen X, Zhang D, Yan T, Zhang J, Shi L. Three-dimensional graphene-based hierarchically porous carbon composites prepared by a dual-template strategy for capacitive

- deionization. *Journal of Materials Chemistry A*. 2013;1(39):12334–12344. DOI: 10.1039/C3TA12683H.
- [35] Huang X, Qian K, Yang J, Zhang J, Li L, Yu C, Zhao D. Functional nanoporous graphene foams with controlled pore sizes. *Advanced Materials*. 2012;24(32):4419–4423. DOI: 10.1002/adma.201201680.
- [36] Choi BG, Yang M, Hong WH, Choi JW, Huh YS. 3D macroporous graphene frameworks for supercapacitors with high energy and power densities. *ACS Nano*. 2012;6(5):4020–4028. DOI: 10.1021/nn3003345.
- [37] Cao X, Shi Y, Shi W, Lu G, Huang X, Yan Q, Zhang Q, Zhang H. Preparation of novel 3D graphene networks for supercapacitor applications. *Small*. 2011;7(22):3163–3168. DOI: 10.1002/smll.201100990.
- [38] Dong X-C, Xu H, Wang X-W, Huang Y-X, Chan-Park MB, Zhang H, Wang L-H, Huang W, Chen P. 3D Graphene–cobalt oxide electrode for high-performance supercapacitor and enzymeless glucose detection. *ACS Nano*. 2012;6(4):3206–3213. DOI: 10.1021/nn300097q.
- [39] Maiyalagan T, Dong X, Chen P, Wang X. Electrodeposited Pt on three-dimensional interconnected graphene as a free-standing electrode for fuel cell application. *Journal of Materials Chemistry*. 2012;22(12):5286–5290. DOI: 10.1039/C2JM16541D.
- [40] Yong Y-C, Dong X-C, Chan-Park MB, Song H, Chen P. Macroporous and monolithic anode based on polyaniline hybridized three-dimensional graphene for high-performance microbial fuel cells. *ACS Nano*. 2012;6(3):2394–2400. DOI: 10.1021/nn204656d.
- [41] Qiu H, Dong X, Sana B, Peng T, Paramelle D, Chen P, Lim S. Ferritin-templated synthesis and self-assembly of Pt nanoparticles on a monolithic porous graphene network for electrocatalysis in fuel cells. *ACS Applied Materials & Interfaces*. 2013;5(3):782–787. DOI: 10.1021/am3022366.
- [42] Wang M, Fu L, Gan L, Zhang C, Rummeli M, Bachmatiuk A, Huang K, Fang Y, Liu Z. CVD Growth of large area smooth-edged graphene nanomesh by nanosphere lithography. *Scientific Reports*. 2013;3:1238. DOI: 10.1038/srep01238. <http://www.nature.com/articles/srep01238#supplementary-information>
- [43] Chen Z, Xu C, Ma C, Ren W, Cheng H-M. Lightweight and flexible graphene foam composites for high-performance electromagnetic interference shielding. *Advanced Materials*. 2013;25(9):1296–1300. DOI: 10.1002/adma.201204196.
- [44] Chen Z, Ren W, Gao L, Liu B, Pei S, Cheng H-M. Three-dimensional flexible and conductive interconnected graphene networks grown by chemical vapour deposition. *Nature Material*. 2011;10(6):424–428. DOI: <http://www.nature.com/nmat/journal/v10/n6/abs/nmat3001.html#supplementary-information>
- [45] Chen C-M, Zhang Q, Huang C-H, Zhao X-C, Zhang B-S, Kong Q-Q, Wang M-Z, Yang Y-G, Cai R, Sheng Su D. Macroporous 'bubble' graphene film via template-directed

- ordered-assembly for high rate supercapacitors. *Chemical Communications*. 2012;48(57):7149–7151. DOI: 10.1039/C2CC32189K.
- [46] Zhu Y, Murali S, Stoller MD, Ganesh KJ, Cai W, Ferreira PJ, Pirkle A, Wallace RM, Cychosz KA, Thommes M, Su D, Stach EA, Ruoff RS. Carbon-based supercapacitors produced by activation of graphene. *Science*. 2011;332(6037):1537–1541. DOI: 10.1126/science.1200770.
- [47] Lillo-Ródenas MA, Cazorla-Amorós D, Linares-Solano A. Understanding chemical reactions between carbons and NaOH and KOH: an insight into the chemical activation mechanism. *Carbon*. 2003;41(2):267–275. DOI: [http://dx.doi.org/10.1016/S0008-6223\(02\)00279-8](http://dx.doi.org/10.1016/S0008-6223(02)00279-8).
- [48] Rui X, Zhu J, Sim D, Xu C, Zeng Y, Hng HH, Lim TM, Yan Q. Reduced graphene oxide supported highly porous V_2O_5 spheres as a high-power cathode material for lithium ion batteries. *Nanoscale*. 2011;3(11):4752–4758. DOI: 10.1039/C1NR10879D.
- [49] Chen Y, Wang Q, Zhu C, Gao P, Ouyang Q, Wang T, Ma Y, Sun C. Graphene/porous cobalt nanocomposite and its noticeable electrochemical hydrogen storage ability at room temperature. *Journal of Materials Chemistry*. 2012;22(13):5924–5927. DOI: 10.1039/C2JM16825A.
- [50] Lee JM, Kim IY, Han SY, Kim TW, Hwang S-J. Graphene nanosheets as a platform for the 2D ordering of metal oxide nanoparticles: mesoporous 2D aggregate of anatase TiO_2 nanoparticles with improved electrode performance. *Chemistry – A European Journal*. 2012;18(43):13800–13809. DOI: 10.1002/chem.201200551.
- [51] Yan J, Sun W, Wei T, Zhang Q, Fan Z, Wei F. Fabrication and electrochemical performances of hierarchical porous $Ni(OH)_2$ nanoflakes anchored on graphene sheets. *Journal of Materials Chemistry*. 2012;22(23):11494–11502. DOI: 10.1039/C2JM30221G.
- [52] Yang S, Sun Y, Chen L, Hernandez Y, Feng X, Müllen K. Porous iron oxide ribbons grown on graphene for high-performance lithium storage. *Scientific Reports*. 2012;2:427. DOI: 10.1038/srep00427. <http://www.nature.com/articles/srep00427#supplementary-information>.
- [53] Zheng M, Qiu D, Zhao B, Ma L, Wang X, Lin Z, Pan L, Zheng Y, Shi Y. Mesoporous iron oxide directly anchored on a graphene matrix for lithium-ion battery anodes with enhanced strain accommodation. *RSC Advances*. 2013;3(3):699–703. DOI: 10.1039/C2RA22702A.
- [54] Liu J, Cai H, Yu X, Zhang K, Li X, Li J, Pan N, Shi Q, Luo Y, Wang X. Fabrication of graphene nanomesh and improved chemical enhancement for Raman Spectroscopy. *The Journal of Physical Chemistry C*. 2012;116(29):15741–15746. DOI: 10.1021/jp303265d.

- [55] Yan Y, Yin Y-X, Xin S, Guo Y-G, Wan L-J. Ionothermal synthesis of sulfur-doped porous carbons hybridized with graphene as superior anode materials for lithium-ion batteries. *Chemical Communications*. 2012;48(86):10663–10665. DOI: 10.1039/C2CC36234A.
- [56] Nardecchia S, Carriazo D, Ferrer ML, Gutierrez MC, del Monte F. Three dimensional macroporous architectures and aerogels built of carbon nanotubes and/or graphene: synthesis and applications. *Chemical Society Reviews*. 2013;42(2):794–830. DOI: 10.1039/C2CS35353A.
- [57] Li C, Shi G. Functional gels based on chemically modified graphenes. *Advanced Materials*. 2014;26(24):3992–4012. DOI: 10.1002/adma.201306104.
- [58] Chabot V, Higgins D, Yu A, Xiao X, Chen Z, Zhang J. A review of graphene and graphene oxide sponge: material synthesis and applications to energy and the environment. *Energy & Environmental Science*. 2014;7(5):1564–1596. DOI: 10.1039/C3EE43385D.
- [59] Wu D, Zhang F, Liang H, Feng X. Nanocomposites and macroscopic materials: assembly of chemically modified graphene sheets. *Chemical Society Reviews*. 2012;41(18):6160–6177. DOI: 10.1039/C2CS35179J.
- [60] Xu Y, Sheng K, Li C, Shi G. Self-assembled graphene hydrogel via a one-step hydrothermal process. *ACS Nano*. 2010;4(7):4324–4330. DOI: 10.1021/nn101187z.
- [61] Zhang L, Shi G. Preparation of highly conductive graphene hydrogels for fabricating supercapacitors with high rate capability. *The Journal of Physical Chemistry C*. 2011;115(34):17206–17212. DOI: 10.1021/jp204036a.
- [62] Tarascon JM, Armand M. Issues and challenges facing rechargeable lithium batteries. *Nature*. 2001;414(6861):359–367.
- [63] Aleksandrak M, Mijowska E, Graphene and its derivatives for energy storage. In: *Graphene Materials*. 2015, A. Tiwari and M. Syväjärvi. Hoboken, NJ, USA John Wiley & Sons, Inc. p. 191–224.
- [64] Adelhelm P, Hu YS, Chuenchom L, Antonietti M, Smarsly BM, Maier J. Generation of hierarchical meso- and macroporous carbon from mesophase pitch by spinodal decomposition using polymer templates. *Advanced Materials*. 2007;19(22):4012–4017. DOI: 10.1002/adma.200700699.
- [65] Wang H, Cui L-F, Yang Y, Sanchez Casalongue H, Robinson JT, Liang Y, Cui Y, Dai H. Mn_3O_4 -graphene hybrid as a high-capacity anode material for lithium ion batteries. *Journal of the American Chemical Society*. 2010;132(40):13978–13980. DOI: 10.1021/ja105296a.
- [66] Li B, Cao H, Shao J, Li G, Qu M, Yin G. Co_3O_4 @graphene composites as anode materials for high-performance lithium ion batteries. *Inorganic Chemistry*. 2011;50(5):1628–1632. DOI: 10.1021/ic1023086.

- [67] Zhou G, Wang D-W, Li F, Zhang L, Li N, Wu Z-S, Wen L, Lu GQ, Cheng H-M. Graphene-wrapped Fe_3O_4 anode material with improved reversible capacity and cyclic stability for lithium ion batteries. *Chemistry of Materials*. 2010;22(18):5306–5313. DOI: 10.1021/cm101532x.
- [68] Zhuo L, Wu Y, Wang L, Ming J, Yu Y, Zhang X, Zhao F. CO_2 -expanded ethanol chemical synthesis of a Fe_3O_4 @graphene composite and its good electrochemical properties as anode material for Li-ion batteries. *Journal of Materials Chemistry A*. 2013;1(12):3954–3960. DOI: 10.1039/C3TA01388J.
- [69] Chen W, Li S, Chen C, Yan L. Self-assembly and embedding of nanoparticles by in situ reduced graphene for preparation of a 3D graphene/nanoparticle aerogel. *Advanced Materials*. 2011;23(47):5679–5683. DOI: 10.1002/adma.201102838.
- [70] Goodenough JB, Kim Y. Challenges for rechargeable Li batteries. *Chemistry of Materials*. 2010;22(3):587–603. DOI: 10.1021/cm901452z.
- [71] Manthiram A. Materials challenges and opportunities of lithium ion batteries. *The Journal of Physical Chemistry Letters*. 2011;2(3):176–184. DOI: 10.1021/jz1015422.
- [72] Kim H, Lim H-D, Kim J, Kang K. Graphene for advanced Li/S and Li/air batteries. *Journal of Materials Chemistry A*. 2014;2(1):33–47. DOI: 10.1039/C3TA12522J.
- [73] Yu M, Li R, Wu M, Shi G. Graphene materials for lithium–sulfur batteries. *Energy Storage Materials*. 2015;1:51–73. DOI: <http://dx.doi.org/10.1016/j.ensm.2015.08.004>.
- [74] Manthiram A, Fu Y, Chung S-H, Zu C, Su Y-S. Rechargeable lithium–sulfur batteries. *Chemical Reviews*. 2014;114(23):11751–11787. DOI: 10.1021/cr500062v.
- [75] Manthiram A, Chung S-H, Zu C. Lithium–sulfur batteries: progress and prospects. *Advanced Materials*. 2015;27(12):1980–2006. DOI: 10.1002/adma.201405115.
- [76] Lin Z, Liang C. Lithium-sulfur batteries: from liquid to solid cells. *Journal of Materials Chemistry A*. 2015;3(3):936–958. DOI: 10.1039/C4TA04727C.
- [77] Wang J-Z, Lu L, Choucair M, Stride JA, Xu X, Liu H-K. Sulfur-graphene composite for rechargeable lithium batteries. *Journal of Power Sources*. 2011;196(16):7030–7034. DOI: <http://dx.doi.org/10.1016/j.jpowsour.2010.09.106>.
- [78] Wang B, Li K, Su D, Ahn H, Wang G. Superior electrochemical performance of sulfur/graphene nanocomposite material for high-capacity lithium–sulfur batteries. *Chemistry – An Asian Journal*. 2012;7(7):1637–1643. DOI: 10.1002/asia.201200004.
- [79] Kim KH, Jun Y-S, Gerbec JA, See KA, Stucky GD, Jung H-T. Sulfur infiltrated mesoporous graphene–silica composite as a polysulfide retaining cathode material for lithium–sulfur batteries. *Carbon*. 2014;69:543–551. DOI: <http://dx.doi.org/10.1016/j.carbon.2013.12.065>.

- [80] Zheng S, Wen Y, Zhu Y, Han Z, Wang J, Yang J, Wang C. In situ sulfur reduction and intercalation of graphite oxides for Li-S battery cathodes. *Advanced Energy Materials*. 2014;4(16):n/a-n/a. DOI: 10.1002/aenm.1400482-1 to 1400482-9.
- [81] Ding B, Yuan C, Shen L, Xu G, Nie P, Lai Q, Zhang X. Chemically tailoring the nanostructure of graphene nanosheets to confine sulfur for high-performance lithium-sulfur batteries. *Journal of Materials Chemistry A*. 2013;1(4):1096-1101. DOI: 10.1039/C2TA00396A.
- [82] Evers S, Nazar LF. Graphene-enveloped sulfur in a one pot reaction: a cathode with good coulombic efficiency and high practical sulfur content. *Chemical Communications*. 2012;48(9):1233-1235. DOI: 10.1039/C2CC16726C.
- [83] Sun H, Xu G-L, Xu Y-F, Sun S-G, Zhang X, Qiu Y, Yang S. A composite material of uniformly dispersed sulfur on reduced graphene oxide: aqueous one-pot synthesis, characterization and excellent performance as the cathode in rechargeable lithium-sulfur batteries. *Nano Research*. 2012;5(10):726-738. DOI: 10.1007/s12274-012-0257-7.
- [84] Gao X, Li J, Guan D, Yuan C. A scalable graphene sulfur composite synthesis for rechargeable lithium batteries with good capacity and excellent coulombic efficiency. *ACS Applied Materials & Interfaces*. 2014;6(6):4154-4159. DOI: 10.1021/am4057979.
- [85] Simon P, Gogotsi Y. Materials for electrochemical capacitors. *Nature Material* 2008;7(11):845-854.
- [86] Liu C, Li F, Ma L-P, Cheng H-M. Advanced materials for energy storage. *Advanced Materials*. 2010;22(8):E28-E62. DOI: 10.1002/adma.200903328.
- [87] Zhai Y, Dou Y, Zhao D, Fulvio PF, Mayes RT, Dai S. Carbon materials for chemical capacitive energy storage. *Advanced Materials*. 2011;23(42):4828-4850. DOI: 10.1002/adma.201100984.
- [88] Zhang X, Zhang H, Li C, Wang K, Sun X, Ma Y. Recent advances in porous graphene materials for supercapacitor applications. *RSC Advances*. 2014;4(86):45862-45884. DOI: 10.1039/C4RA07869A.
- [89] Stoller MD, Park S, Zhu Y, An J, Ruoff RS. Graphene-based ultracapacitors. *Nano Letters*. 2008;8(10):3498-3502. DOI: 10.1021/nl802558y.
- [90] Chen Y, Zhang X, Zhang H, Sun X, Zhang D, Ma Y. High-performance supercapacitors based on a graphene-activated carbon composite prepared by chemical activation. *RSC Advances*. 2012;2(20):7747-7753. DOI: 10.1039/C2RA20667F.
- [91] Zhang L, Zhang F, Yang X, Long G, Wu Y, Zhang T, Leng K, Huang Y, Ma Y, Yu A, Chen Y. Porous 3D graphene-based bulk materials with exceptional high surface area and excellent conductivity for supercapacitors. *Scientific Reports*. 2013;3:1408. DOI: 10.1038/srep01408. <http://www.nature.com/articles/srep01408#supplementary-information>.

- [92] Jeong HM, Lee JW, Shin WH, Choi YJ, Shin HJ, Kang JK, Choi JW. Nitrogen-doped graphene for high-performance ultracapacitors and the importance of nitrogen-doped sites at basal planes. *Nano Letters*. 2011;11(6):2472–2477. DOI: 10.1021/nl2009058.
- [93] Wu Z-S, Ren W, Xu L, Li F, Cheng H-M. Doped graphene sheets as anode materials with superhigh rate and large capacity for lithium ion batteries. *ACS Nano*. 2011;5(7):5463–5471. DOI: 10.1021/nn2006249.
- [94] Wang S, Iyyamperumal E, Roy A, Xue Y, Yu D, Dai L. Vertically aligned BCN nanotubes as efficient metal-free electrocatalysts for the oxygen reduction reaction: a synergetic effect by co-doping with boron and nitrogen. *Angewandte Chemie International Edition*. 2011;50(49):11756–11760. DOI: 10.1002/anie.201105204.
- [95] Qiu Y, Zhang X, Yang S. High performance supercapacitors based on highly conductive nitrogen-doped graphene sheets. *Physical Chemistry Chemical Physics*. 2011;13(27):12554–12558. DOI: 10.1039/C1CP21148J.
- [96] Wu Z-S, Winter A, Chen L, Sun Y, Turchanin A, Feng X, Müllen K. Three-dimensional nitrogen and boron co-doped graphene for high-performance all-solid-state supercapacitors. *Advanced Materials*. 2012;24(37):5130–5135. DOI: 10.1002/adma.201201948.
- [97] Wu Z-S, Sun Y, Tan Y-Z, Yang S, Feng X, Müllen K. Three-dimensional graphene-based macro- and mesoporous frameworks for high-performance electrochemical capacitive energy storage. *Journal of the American Chemical Society*. 2012;134(48):19532–19535. DOI: 10.1021/ja308676h.
- [98] Xu C, Li J, Wang X, Wang J, Wan L, Li Y, Zhang M, Shang X, Yang Y. Synthesis of hemin functionalized graphene and its application as a counter electrode in dye-sensitized solar cells. *Materials Chemistry and Physics*. 2012;132(2–3):858–864. DOI: <http://dx.doi.org/10.1016/j.matchemphys.2011.12.025>
- [99] Yen M-Y, Hsieh C-K, Teng C-C, Hsiao M-C, Liu P-I, Ma C-CM, Tsai M-C, Tsai C-H, Lin Y-R, Chou T-Y. Metal-free, nitrogen-doped graphene used as a novel catalyst for dye-sensitized solar cell counter electrodes. *RSC Advances*. 2012;2(7):2725–2728. DOI: 10.1039/C2RA00970F.
- [100] Xue Y, Liu J, Chen H, Wang R, Li D, Qu J, Dai L. Nitrogen-doped graphene foams as metal-free counter electrodes in high-performance dye-sensitized solar cells. *Angewandte Chemie International Edition*. 2012;51(48):12124–12127. DOI: 10.1002/anie.201207277.